Res Chem Intermed
DOI 10.1007/s11164-015-2176-1

Synthesis, biological evaluation and molecular docking studies of *N*-acylheteroaryl hydrazone derivatives as antioxidant and anti-inflammatory agents

Pravin S. Mahajan[1] · Mukesh D. Nikam[1] · Vijay M. Khedkar[2] · Prakash C. Jha[3] · Dhiman Sarkar[2] · Charansingh H. Gill[1]

Received: 15 April 2015 / Accepted: 13 July 2015

Abstract In search of new therapeutics with greater potency, three new series of 3-methyl-1-phenyl-1*H*-thieno[2,3-*c*]pyrazole-5-carbohydrazide derivatives have been synthesized and evaluated for their in vitro antioxidant and anti-inflammatory activities. The hydrazones bearing a core pyrazole, chromone and tetrazolo[1,5-*a*]quinoline scaffold showed promising activities. Interestingly, compounds **3a** ($EC_{50} = 06.00 \pm 2.36$) and **5c** ($EC_{50} = 07.21 \pm 0.67$) showed the most potent antioxidant activity, while compounds **3a** ($EC_{50} = 10.25 \pm 1.08$), **7b** ($EC_{50} = 10.50 \pm 0.99$) and **7c** ($EC_{50} = 11.18 \pm 0.15$) showed significant anti-inflammatory activity. Furthermore, molecular docking studies also revealed a significant correlation between the binding score and biological activity for these compounds to describe the molecular basis for the structure activity relationship (SAR) results. As these compounds are good cyclooxygenase inhibitors, isoenzyme inhibitory potency studies are warranted.

Keywords *N*-Acylhydrazones · Anti-inflammatory · Antioxidant · Docking study · Structure–activity relationship

✉ Charansingh H. Gill
chgill16@gmail.com

[1] Department of Chemistry, Dr. Babasaheb Ambedkar Marathwada University, Aurangabad, Maharashtra 431 004, India

[2] Combi-Chem Resource Centre, CSIR-National Chemical Laboratory, Pune 411008, India

[3] School of Chemical Sciences, Central University of Gujarat, Sector-30, Gandhinagar 38200, Gujarat, India

Published online: 29 July 2015

Introduction

The main aim of therapeutics is to relieve pain and minimize side effects. In this respect, antioxidants are important to maintain health and to cure diseases [1]. In various pathophysiological conditions, excessive generation of reactive oxygen species (ROSs) results in oxidative stress. Antioxidants attract much attention as aging, cancer, atherosclerosis, and some other serious diseases have been confirmed to correlate with low density lipoprotein (LDL), cell membranes, and DNA exposed to oxidative stress [2, 3].

Nonsteroidal anti-inflammatory drugs (NSAIDs) relieve pain and inflammation [4] by inhibiting the enzyme prostaglandin endoperoxidase, popularly known as cyclooxygenase-2 (COX-2) [5], thereby blocking the biosynthesis of prostaglandin [6]. It is well known that NSAIDs are associated with several side effects such as gastrointestinal mucosal damage, bleeding, intolerance, renal toxicity [7] and dyspepsia [8]. Several attempts were made to improve the safety of existing NSAIDs, including the use of coating or encapsulation, and the use of rectal or topical formulations [9–11], but an ideal solution to the problem was not achieved. Therefore, current research focuses on production of new, improved non-opioid analgesics similar to opioids but without their side effects, and with improved activity.

ROSs produced by phagocytic leukocytes (e.g., neutrophils, monocytes, macrophages, eosinophils) during the inflammatory process invade tissues [12]. Neutrophils play a key role in inflammatory response and also generate a toxic oxygen metabolite including ROSs by various pathways [13, 14] and it is well known that free radicals play an important role in inflammatory action [15]. Thus, the agents that can scavenge these ROSs can be of assistance in the treatment of inflammatory disorders.

N-acylhydrazones (NAHs) are stable imine equivalents which provides a suitable template for the chelation of Lewis acids [16], and are expanded to the chemical and pharmaceutical industries [17]. The pyrazole ring is a predominant pharmacophore in many drugs such as celecoxib, pyrazofurin and, notably, rimonabant, having a pyrazole core with *N*-acylhydrazone. The bioactive system containing thieno[2,3-*c*]pyrazole derivatives are a class of fused heterocyclic compounds which have attracted interest in medicinal chemistry owing to their antitumor [18–22], antiviral [23], anti-inflammatory [24] activities. Several other compounds containing the thieno[2,3-*c*]pyrazole scaffold were described as inhibitory for phosphodiesterase 7A (PDE7A) [25] and as potassium channel inhibitors [26].

A literature survey reveals that some pharmacophores like chromones and their hydrazone derivatives possess potential antioxidant and anti-inflammatory activities [27, 28]. The tetrazolo[1,5-*a*]quinoline nucleus with hydrazones [29] and a few pyrazole carbohydrazide hydrazone derivatives serve as new scaffolds for anti-inflammatory activity [30–32]. However, there have been no reports on the synthesis and biological evaluation of 3-methyl-1-phenyl-1*H*-thieno[2,3-*c*]pyrazole-5-carbohydrazide hydrazone derivatives.

With the hope of greater potency, additional pharmacokinetic advantages and our continuous attention towards synthesis of biologically active heterocyclic compounds [33–35], we thought of preparing new hydrazone derivatives in order to screen them for antioxidant and anti-inflammatory activities. Anti-inflammatory activities shown by the compounds investigated herein motivated us to evaluate whether they are a good ligand to the known target protein related to inflammation, i.e., cyclooxygenase-2. We have tried to understand the interactions involved in the binding of these compounds to cyclooxygenase-2 via computational docking methods for gaining insights into the experimentally observed inhibition pattern.

Experimental

Materials and methods

The melting points of all synthesized compounds were determined by an open capillary method and were uncorrected. All chemicals were analytical grade and used without further purification. Precoated plates (silica gel 60 F_{254}) were used for analytical thin-layer chromatography (TLC) for monitoring the reaction progress, and spots were visualized with ultraviolet (UV) light and iodine. Infrared (IR) spectra (KBr disc) were recorded on a Jasco Fourier transform-infrared (FTIR-4100) spectrometer (Japan). Proton nuclear magnetic resonance (^{1}H NMR) spectra were recorded on a Bruker Advance II 400 MHz spectrometer in deuterated dimethylsilane (DMSO-d_6 ; δ in ppm relative to tetramethylsilane). Carbon nuclear magnetic resonance (^{13}C NMR) spectra were recorded on a Bruker Advance II 100 MHz spectrometer in DMSO-d_6. Mass spectra were recorded on a Q-Tof micro mass spectrometer (Waters Corporation) by the electro-spray (ES) method. Elemental analysis was performed on Perkin-Elmer EAL-240 elemental analyzer.

Substituted tetrazolo[1,5-*a*]quinoline-4-carbaldehyde (**2a–2g**), 1,3-diphenyl-1*H*-pyrazole-4-carbaldehyde (**4a–h**) and 3-formylchromone (**6a–d**) were prepared in accordance with Refs. [8, 36, 37], respectively.

General procedure for the synthesis of hydrazones (3a–g)

The carbohydrazide **1** (1 mmol) and substituted tetrazolo[1,5-*a*]quinoline-4-carbaldehyde (**2a-g**) (1 mmol) were added in methanol with a few drops of acetic acid with stirring for 15-30 min. (monitored by TLC) at room temperature. After completion of the reaction, the reaction mixture was poured on crushed ice. The resulting crude product was purified by column chromatography on silica gel by EtOAc:petroleum ether (9:1) as an eluent to afford the pure title compounds **3a–g**.

(E)-N′-((7-ethoxytetrazolo[1,5-a]quinolin-4-yl)methylene)-3-methyl-1-phenyl-1H-thieno[2,3-c]pyrazole-5-carbohydrazide (3a) Yellow solid, m.p. 240–242 °C, Yield: 75 %. IR (KBr, cm^{-1}): 3444 (NH), 3063, 2927 (Ar–CH), 1636 (amide C=O), 1614 (C=N). ^{1}H NMR (400 MHz, DMSO-d_6, δ, ppm): 1.32 (t, 3H, CH_3), 2.54 (s, 3H, CH_3), 4.06 (q, 2H, OCH_2), 7.12 (s, 1H), 7.21-7.78 (m, 5H, Ar–H), 7.54 (d, 1H,

Ar–H), 8.12 (s, 1H, thiophene-H), 8.38 (d, 1H), 8.58 (s, 1H), 9.02 (s. 1H, CH=N), 11.89 (s, 1H, NH). ^{13}C NMR (100 MHz, DMSO-d_6, δ, ppm): 12.90, 14.22, 61.63, 107.13, 116.20, 116.50, 123.51, 124.21, 125.12, 129.60, 130.40, 130.72, 131.13, 132.90, 135.25, 137.29, 138.11, 141.05, 142.91, 144.13, 147.89, 149.01, 159.41, 162.50. High resolution mass spectroscopy (HRMS) (ESI+) *m/z*: $(M + H)^+$ calcd. for $C_{25}H_{20}N_8O_2S$ 497.1504, found 497.1488. Anal. calcd. for $C_{25}H_{20}N_8O_2S$: C, 60.47; H, 4.06; N, 22.57; S, 6.46; found: C, 60.22; H, 3.90; N, 22.87; S, 6.28.

(E)-3-methyl-1-phenyl-N′-(tetrazolo[1,5-a]quinolin-4-ylmethylene)-1H-thieno[2,3-c]pyrazole-5-carbohydrazide (3b) Yellow solid, m.p. 261–264 °C, Yield: 77 %. IR (KBr, cm^{-1}): 3446 (NH), 3076, 2929 (Ar–CH), 1630 (amide C=O), 1606 (C=N). ^{1}H NMR (400 MHz, DMSO-d_6, δ, ppm): 2.51 (s, 3H, CH_3), 7.07–7.80 (m, 5H, Ar–H), 8.01 (dd, 1H), 8.07 (dd, 1H), 8.16 (s, 1H, thiophene-H), 8.26 (d, 1H), 8.46 (d, 1H), 8.51 (s, 1H), 9.00 (s. 1H, CH=N), 11.91 (s, 1H, NH). ^{13}C NMR (100 MHz, DMSO-d_6, δ, ppm): 12.96, 116.22, 116.60, 116.91, 123.39, 125.05, 125.08, 127.51, 128.03, 129.06, 129.09, 130.08, 133.31, 135.08, 138.70, 141.42, 143.63, 146.01, 147.07, 151.31, 161.90. HRMS (ESI+) *m/z*: $(M + H)^+$ calcd. for $C_{23}H_{16}N_8OS$ 453.1619, found 453.1616. Anal. calcd. for $C_{23}H_{16}N_8OS$: C, 61.05; H, 3.56; N, 24.76; S, 7.09; found: C, 61.10; H, 3.72; N, 24.61; S, 7.13.

(E)-N′-((8-methoxytetrazolo[1,5-a]quinolin-4-yl)methylene)-3-methyl-1-phenyl-1H-thieno[2,3-c]pyrazole-5-carbohydrazide (3c) Yellow solid, m.p. 242–244 °C, Yield: 72 %. IR (KBr, cm^{-1}): 3458 (NH), 3066, 2921 (Ar–CH), 1630 (amide C=O), 1612 (C=N). ^{1}H NMR (400 MHz, DMSO-d_6, δ, ppm): 2.56 (s, 3H, CH_3), 3.74 (s, 3H, OCH_3), 7.22-7.84 (m, 5H, Ar–H), 7.30 (s, 1H, Ar–H), 7.42 (d, 1H, Ar–H), 8.18 (d, 1H), 8.55 (s, 1H), 9.02 (s. 1H, CH=N), 11.91 (s, 1H, NH). ^{13}C NMR (100 MHz, DMSO-d_6, δ, ppm): 13.00, 55.61, 109.09, 116.25, 116.91, 119.21, 122.41, 125.92, 126.11, 129.88, 130.39, 131.10, 135.58, 137.61, 138.02, 141.89, 143.18, 144.51, 150.02, 152.08, 158.61, 163.11. HRMS (ESI+) *m/z*: $(M + H)^+$ calcd for $C_{24}H_{18}N_8OS$ 483.1347, found 483.1327. Anal. calcd. for $C_{24}H_{18}N_8OS$: C, 59.74; H, 3.76; N, 23.22; S, 6.65; found: C, 59.63; H, 3.80; N, 23.48; S, 6.87.

(E)-3-methyl-N′-((7-methyltetrazolo[1,5-a]quinolin-4-yl)methylene)-1-phenyl-1H-thieno[2,3-c]pyrazole-5-carbohydrazide (3d) Yellow solid, m.p. 206–208 °C, Yield: 79 %. IR (KBr, cm^{-1}): 3463 (NH), 3084, 2928 (Ar–CH), 1646 (amide C=O), 1610 (C=N). ^{1}H NMR (400 MHz, DMSO-d_6, δ, ppm): 2.34 (s, 3H, CH_3), 2.48 (s, 3H, CH_3), 7.21–7.74 (m, 5H, Ar–H), 7.66 (s, 1H, Ar–H), 7.98 (d, 1H, Ar–H), 8.12 (s, 1H, thiophene-H), 8.40 (d, 1H), 8.58 (s, 1H), 9.00 (s. 1H, CH=N), 11.91 (s, 1H, NH). ^{13}C NMR (100 MHz, DMSO-d_6, δ, ppm): 13.02, 21.78, 116.08, 116.71, 125.09, 125.28, 127.19, 128.51, 129.38, 129.91, 130.88, 132.49, 135.41, 136.53, 138.02, 138.79, 141.58, 143.92, 144.73, 148.77, 150.78, 162.29. HRMS (ESI+) *m/z*: $(M + H)^+$ calcd. for $C_{24}H_{18}N_8OS$ 467.1398, found 467.1381. Anal. calcd. for $C_{24}H_{18}N_8OS$: C, 61.79; H, 3.89; N, 24.02; S, 6.87; found: C, 61.95; H, 3.91; N, 23.90; S, 6.94.

*(E)-3-methyl-N′-((8-methyltetrazolo[1,5-a]quinolin-4-yl)methylene)-1-phenyl-1H-thieno[2,3-c]pyrazole-5-carbohydrazide (**3e**)* Yellow solid, m.p. 224–226 °C,

Yield: 75 %. IR (KBr, cm^{-1}): 3448 (NH), 3078, 2928 (Ar–CH), 1638 (amide C=O), 1611 (C=N). ^{1}H NMR (400 MHz, DMSO-d_6, δ, ppm): 2.34 (s, 3H, CH_3), 2.48 (s, 3H, CH_3), 7.19–7.74 (m, 5H, Ar–H), 7.82 (d, 1H, Ar–H), 7.99 (dd, 1H, Ar–H), 8.10 (s, 1H, thiophene-H), 8.22 (d, 1H), 8.57 (s, 1H), 9.01 (s. 1H, CH=N), 11.90 (s, 1H, NH). ^{13}C NMR (100 MHz, DMSO-d_6, δ, ppm): 13.00, 21.78, 115.91, 116.88, 125.21, 125.42, 127.01, 128.77, 129.19, 130.03, 130.81, 132.09, 135.48, 136.69, 138.31, 138.61, 141.92, 143.59, 144.92, 149.01, 151.00, 161.99. HRMS (ESI+) *m/z*: $(M + H)^+$ calcd. for $C_{24}H_{18}N_8OS$ 467.1398, found 467.1381. Anal. calcd. for $C_{24}H_{18}N_8OS$: C, 61.79; H, 3.89; N, 24.02; S, 6.87; found: C, 61.95; H, 3.91; N, 23.90; S, 6.94.

*(E)-3-methyl-N′-((9-methyltetrazolo[1,5-a]quinolin-4-yl)methylene)-1-phenyl-1H-thieno[2,3-c]pyrazole-5-carbohydrazide (**3f**)* Yellow solid, m.p. 230–232 °C, Yield: 78 %. IR (KBr, cm^{-1}): 3450 (NH), 1633 (amide C=O), 1611 (C=N). ^{1}H NMR (400 MHz, DMSO-d_6, δ, ppm): 2.32 (s, 3H, CH_3), 2.51 (s, 3H, CH_3), 7.24–7.74 (m, 5H, Ar–H), 7.90 (dd, 1H, Ar–H), 8.01 (s, 1H, thiophene-H), 8.07 (d, 1H), 8.14 (d, 1H), 8.55 (s, 1H), 8.97 (s. 1H, CH=N), 11.92 (s, 1H, NH). ^{13}C NMR (100 MHz, DMSO-d_6, δ, ppm): 13.02, 21.79, 116.03, 117.08, 125.29, 125.71, 127.00, 128.57, 129.11, 129.67, 131.10, 132.19, 135.58, 136.13, 138.22, 138.90, 142.00, 143.52, 144.08, 148.88, 150.91, 162.08. HRMS (ESI+) *m/z*: $(M + H)^+$ calcd. for $C_{24}H_{18}N_8OS$ 467.1398, found 467.1381. Anal. calcd. for $C_{24}H_{18}N_8OS$: C, 61.79; H, 3.89; N, 24.02; S, 6.87; found: C, 61.95; H, 3.91; N, 23.90; S, 6.94.

(E)-N′-((7-methoxytetrazolo[1,5-a]quinolin-4-yl)methylene)-3-methyl-1-phenyl-1H-thieno[2,3-c]pyrazole-5-carbohydrazide (3g) Yellow solid, m.p. 180–182 °C, Yield: 67 %. IR (KBr, cm^{-1}): 3456 (NH), 3081, 2929 (Ar–CH), 1635 (amide C=O), 1611 (C=N). ^{1}H NMR (400 MHz, DMSO-d_6, δ, ppm): 2.56 (s, 3H, CH_3), 3.84 (s, 3H, OCH_3), 7.16 (s, 1H, Ar–H), 7.25–7.84 (m, 5H, Ar–H), 7.44 (d, 1H, Ar–H), 8.14 (s, 1H, thiophene-H), 8.35 (d, 1H), 8.60 (s, 1H), 9.02 (s. 1H, CH=N), 11.91 (s, 1H, NH). ^{13}C NMR (100 MHz, DMSO-d_6, δ, ppm): 13.01, 55.85, 108.91, 116.42, 117.13, 119.02, 122.08, 125.82, 126.29, 130.01, 130.60, 131.32, 135.51, 137.91, 138.23, 142.15, 143.44, 144.41, 150.19, 152.20, 158.69, 163.02. HRMS (ESI+) *m/z*: $(M + H)^+$ calcd. for $C_{25}H_{20}N_4O_3S$ 483.1347, found 483.1327. Anal. calcd. for $C_{25}H_{20}N_4O_3S$: C, 59.74; H, 3.76; N, 23.22; S, 6.65; found: C, 59.63; H, 3.80; N, 23.48; S, 6.87.

General procedure for the synthesis of hydrazones (5a–h)

To a stirred solution of carbohydrazide **1** (1 mmol) in methanol, was added an equimolar amount of the appropriate 1,3-diphenyl-1*H*-pyrazole-4-carbaldehyde derivatives (**4a–h**) with a few drops of acetic acid. The reaction mixture was stirred at room temperature, until TLC indicated the end of reaction (15–30 min). After completion of the reaction, the reaction mixture was poured on crushed ice. The resulting crude product was purified by column chromatography on silica gel by EtOAc:petroleum ether (8:2) as an eluent to afford the pure title compounds **5a–h**.

(E)-N′-((1,3-diphenyl-1H-pyrazol-4-yl)methylene)-3-methyl-1-phenyl-1H-thieno[2,3-c]pyrazole-5-carbohydrazide (5a) Yellow solid, m.p. 210–212 °C, Yield: 65 %. IR (KBr, cm^{-1}): 3260 (NH), 2924 (Aromatic C–H), 1650 (C=O), 1608 (C=N). ^{1}H NMR (400 MHz, DMSO-d_6, δ, ppm): 2.48 (s, 3H, CH_3), 7.17–7.72 (m, 15H, Ar–H), 8.18 (s, 1H, thiophene-H), 8.38 (s, 1H), 9.36 (s, 1H, CH=N), 11.35 (brs, 1H, NH). ^{13}C NMR (100 MHz, DMSO-d_6, δ, ppm): 12.98, 114.60, 116.64, 116.89, 120.70, 125.52, 127.80, 128.38, 129.01, 129.77, 129.95, 130.30, 130.85, 131.10, 132.83, 135.83, 138.41, 138.67, 141.43, 143.62, 144.50, 152.21, 163.05. HRMS (ESI+) *m/z*: $(M + H)^+$ calcd. for $C_{29}H_{22}N_6OS$ 503.1652, found 503.1656. Anal. calcd. for $C_{29}H_{22}N_6OS$: C, 69.30; H, 4.41; N, 16.72; S, 6.38; found: C, 69.52; H, 4.44; N, 16.51; S, 6.08.

(E)-3-methyl-N′-((3-(4-nitrophenyl)-1-phenyl-1H-pyrazol-4-yl)methylene)-1-phenyl-1H-thieno[2,3-c]pyrazole-5-carbohydrazide (5b) Yellow solid, m.p. 283–285 °C, Yield: 72 %. IR (KBr, cm^{-1}): 3258 (NH), 2924 (Aromatic C–H), 1650 (C=O), 1605 (C=N), 1526 (NO_2, anti), 1507, 1393 (NO_2, sym), 1252, 748, 509. ^{1}H NMR (400 MHz, DMSO-d_6, δ, ppm): 2.39 (s, 3H, CH_3), 7.18-7.22(dd, 2H, Ar–H), 7.46–7.84 (m, 10H, Ar–H), 8.02–8.05 (dd, 2H, Ar–H), 8.22 (s, 1H, thiophene-H), 8.35 (s, 1H), 9.41 (s, 1H, CH=N), 11.45 (brs, 1H, NH). ^{13}C NMR (100 MHz, DMSO-d_6, δ, ppm): 12.99, 114.70, 116.61, 116.93, 120.89, 125.52, 125.88, 126.80, 127.89, 129.94, 130.09, 130.88, 131.28, 135.81, 138.18, 138.73, 140.21, 141.44, 143.62, 144.40, 146.11, 152.29, 163.01. HRMS (ESI+) *m/z*: $(M + H)^+$ calcd. for $C_{29}H_{21}N_7O_3S$ 548.1503, found 548.1509. Anal. calcd. for $C_{29}H_{21}N_7O_3S$: C, 63.61; H, 3.87; N, 17.91; S, 5.86; found: C, 63.33; H, 4.01; N, 18.16; S, 5.50.

(E)-N′-((3-(4-methoxyphenyl)-1-phenyl-1H-pyrazol-4-yl)methylene)-3-methyl-1-phenyl-1H-thieno[2,3-c]pyrazole-5-carbohydrazide (5c) Yellow solid, m.p. 246–248 °C, Yield: 59 %. IR (KBr, cm^{-1}): 3246 (NH), 3043, 2929 (Ar–CH), 1646 (amide C=O), 1599, 1504, 1383, 1338, 858, 743, 665. ^{1}H NMR (400 MHz, DMSO-d_6, δ, ppm): 2.51 (s, 3H, CH_3), 3.78 (s, 3H, OCH_3), 7.04 (d, 2H, Ar–H), 7.20 (d, 2H, Ar–H), 7.40–7.81 (m, 10H, Ar–H), 8.21 (s, 1H, thiophene-H), 8.44 (s, 1H), 9.20 (s, 1H, CH=N), 11.78 (brs, 1H, NH). ^{13}C NMR (100 MHz, DMSO-d_6, δ, ppm): 13.00, 60.47, 114.28, 115.30, 116.61, 116.92, 120.41, 125.55, 126.09, 127.70, 129.23, 129.95, 130.19, 130.84, 131.02, 135.82, 138.30, 138.71, 141.42, 143.62, 144.38, 152.20, 162.09, 163.05. HRMS (ESI+) *m/z*: $(M + H)^+$ calcd for $C_{30}H_{24}N_6O_2S$ 533.1759, found 533.1739. Anal. calcd. for $C_{30}H_{24}N_6O_2S$: C, 67.65; H, 4.54; N, 15.78; S, 6.02; found: C, 67.49; H, 4.58; N, 15.47; S, 6.18.

(E)-N′-((3-(4-fluorophenyl)-1-phenyl-1H-pyrazol-4-yl)methylene)-3-methyl-1-phenyl-1H-thieno[2,3-c]pyrazole-5-carbohydrazide (5d) Yellow solid. m.p. 251–254 °C, Yield: 65 %. IR (KBr, cm^{-1}): 3263 (NH), 1640 (C=O), 1610(C=N). ^{1}H NMR (400 MHz, DMSO-d_6, δ, ppm): 2.44 (s, 3H, CH_3), 7.21–8.05 (m, 14H, Ar–H), 8.22 (s, 1H, thiophene-H), 8.32 (s, 1H), 9.46 (s, 1H, NH), 11.44 (brs, 1H, NH). ^{13}C NMR (100 MHz, DMSO-d_6, δ, ppm): 12.98, 114.52, 116.63, 116.91, 117.13, 120.39, 125.50, 128.07, 129.27, 129.96, 130.10, 130.86, 131.19, 131.38, 135.82, 138.30, 138.68, 141.40, 143.61, 144.10, 152.00, 163.05, 164.00. HRMS (ESI+) *m/z*:

$(M + H)^+$ calcd. for $C_{29}H_{21}FN_6OS$ 521.1558, found 521.1561. Anal. calcd. for $C_{29}H_{21}FN_6OS$: C, 66.91; H, 4.07; N, 16.14; S, 6.16; found: C, 67.12; H, 4.10; N, 15.75; S, 6.02.

(E)-N′-((3-(4-hydroxyphenyl)-1-phenyl-1H-pyrazol-4-yl)methylene)-3-methyl-1-phenyl-1H-thieno[2,3-c]pyrazole-5-carbohydrazide (5e) Yellow solid, m.p. 270–272 °C, Yield: 67 %. IR (KBr, cm^{-1}): 3480 (OH). 3300 (NH), 1670 (C=O), 1600 (C=N). ^1H NMR (400 MHz, DMSO-d_6, δ, ppm): 2.48 (s, 3H, CH_3), 6.86 (d, 2H, Ar–H), 7.44–7.98 (m, 12H, Ar–H), 8.20 (s, 1H, thiophene-H), 8.43 (s, 1H), 9.25 (s. 1H, CH=N), 11.30 (brs, 1H, NH), 14.02 (s, 1H, OH). ^{13}C NMR (100 MHz, DMSO-d_6, δ, ppm): 13.01, 114.48, 116.60, 116.90, 117.19, 120.40, 125.52, 126.10, 127.98, 129.30, 129.95, 130.07, 130.87, 130.90, 135.82, 138.25, 138.70, 141.42, 143.61, 144.06, 152.05, 159.90, 163.01. HRMS (ESI +) *m/z*: $(M + H)^+$ calcd. for $C_{29}H_{22}N_6O_2S$ 519.1601, found 519.1605. Anal. calcd. for $C_{29}H_{22}N_6O_2S$: C, 67.17; H, 4.28; N, 16.21; S, 6.18; found: C, 66.91; H, 4.26; N, 16.50; S, 6.27.

(E)-N′-((3-(4-chlorophenyl)-1-phenyl-1H-pyrazol-4-yl)methylene)-3-methyl-1-phenyl-1H-thieno[2,3-c]pyrazole-5-carbohydrazide (5f) Yellow solid, m.p. 295–297 °C, Yield: 70 %. IR (KBr, cm^{-1}): 3210 (NH), 1665 (C=O), 1600 (C=N). ^1H NMR (400 MHz, DMSO-d_6, δ, ppm): 2.51 (s, 3H, CH_3), 6.91 (d, 2H, Ar–H), 7.41–7.79 (m, 10H, Ar–H), 7.88 (d, 2H, ArH), 8.22 (s, 1H, thiophene-H), 8.44 (s, 1H), 9.40 (s. 1H, CH=N), 11.81 (brs, 1H. NH). ^{13}C NMR (100 MHz, DMSO-d_6, δ, ppm): 13.00, 114.45, 116.61, 116.93, 120.45, 125.53, 127.02, 129.32, 129.94, 130.01, 130.82, 130.86, 131.02, 132.21, 135.82, 136.00, 138.28, 138.72, 141.44, 143.61, 144.04, 152.03, 163.02. HRMS (ESI+) *m/z*: $(M + H)^+$ calcd. for $C_{29}H_{21}ClN_6OS$ 537.1262, found 537.1271. Anal. calcd for $C_{29}H_{21}ClN_6OS$: C, 64.86; H, 3.94; N, 15.65; S, 5.97; found: C, 64.57; H, 4.00; N, 15.75; S, 6.13.

(E)-3-methyl-1-phenyl-N′-((1-phenyl-3-(p-tolyl)-1H-pyrazol-4-yl)methylene)-1H-thieno[2,3-c]pyrazole-5-carbohydrazide (5g) Yellow solid, m.p. 290–291 °C, Yield: 72 %. IR (KBr, cm^{-1}): 3268 (NH), 1645 (C=O), 1618 (C=N). ^1H NMR (400 MHz, DMSO-d_6, δ, ppm): 2.40 (s, 3H, CH_3), 2.61 (s, 3H, CH_3), 7.30–7.82 (m, 14H, Ar–H), 8.21 (s, 1H, thiophene-H), 8.41 (s, 1H), 9.27 (s. 1H, CH=N), 11.30 (brs, 1H, NH). ^{13}C NMR (100 MHz, DMSO-d_6, δ, ppm): 13.00, 21.20, 114.41, 116.63, 116.91, 120.46, 125.54, 127.05, 129.01, 129.35, 129.93, 130.02, 130.82, 130.85, 131.04, 132.23, 135.83, 138.24, 138.71, 141.45, 143.62, 144.6, 152.01, 163.01. HRMS (ESI+) *m/z*: $(M + H)^+$ calcd. for $C_{30}H_{24}N_6OS$ 517.1808, found 517.1822. Anal. calcd. for $C_{30}H_{24}N_6OS$: C, 69.75; H, 4.68; N, 16.27; S, 6.21; found: C, 69.88; H, 4.73; N, 16.09; S, 6.00.

(E)-N′-((3-(4-bromophenyl)-1-phenyl-1H-pyrazol-4-yl)methylene)-3-methyl-1-phenyl-1H-thieno[2,3-c]pyrazole-5-carbohydrazide (5h) Yellow solid, m.p. 295–297 °C, Yield: 60 %, IR (KBr, cm^{-1}): 3252 (NH), 1675 (C=O), 1610 (C=N). ^1H NMR (400 MHz, DMSO-d_6, δ, ppm): 2.43 (s, 3H, CH_3), 7.38–7.88 (m, 14H, Ar–H), 8.20 (s, 1H, thiophene-H), 8.40 (s, 1H), 9.40 (s. 1H, CH=N), 11.40 (brs, 1H, NH). ^{13}C NMR (100 MHz, DMSO-d_6, δ, ppm): 13.00, 114.46, 116.63, 116.90, 121.40, 124.31, 125.56, 127.09, 128.98, 129.92, 130.06, 130.87, 131.02,

132.56, 132.89, 135.82, 138.21, 138.71, 141.46, 143.65, 144.50, 152.48, 163.01. HRMS (ESI+) *m/z*: $(M + H)^+$ calcd. for $C_{29}H_{21}BrN_6OS$ 581.0757, found 581.0780. Anal. calcd. for $C_{29}H_{21}BrN_6OS$: C, 59.90; H, 3.64; N, 14.45; S, 5.51; found: C, 60.15; H, 3.63; N, 14.70; S, 5.37.

General procedure for the synthesis of hydrazones (7a–h)

To a solution of carbohydrazide **1** and substituted 3-formylchromone (**6a–d**) in methanol, was added a few drops of acetic acid with stirring at room temperature with the reaction monitored by TLC (15–30 min). After completion of reaction, the reaction mixture was poured on crushed ice. The resulting crude product was purified by column chromatography on silica gel by EtOAc:petroleum ether (9:1) as an eluent to afford the pure title compounds **7a–h**.

(E)-N′-((7-chloro-4-oxo-4H-chromen-3-yl)methylene)-3-methyl-1-phenyl-1H-thieno[2,3-c]pyrazole-5-carbohydrazide (7a) Yellow solid, m.p. 188–190 °C, Yield: 78 %. IR (KBr, cm^{-1}): 3448 (NH), 3050 (Ar–H), 2922, 1704 (amide C=O), 1642 (pyrone C=O). ^{1}H NMR (400 MHz, DMSO-d_6, δ, ppm): 2.45 (s, 3H, CH_3), 7.26-7.68 (m, 5H, Ar–H), 7.48 (d, 1H), 7.65 (dd, 1H), 8.02 (d, 1H), 8.11 (s, 1H, thiophene-H), 8.25 (s, 1H), 8.60 (s. 1H, CH=N), 10.56 (s, 1H, NH). ^{13}C NMR (100 MHz, DMSO-d_6, δ, ppm): 13.10, 106.08, 116.10, 116.72, 118.03, 123.03, 124.60, 125.15, 125.43, 129.56, 130.46, 135.04, 138.12, 141.47, 143.42, 145.01, 155.05, 157.03, 162.04, 163.44, 176.90. HRMS (ESI+) *m/z*: $(M + H)^+$ calcd. for $C_{23}H_{15}ClN_4O_3S$ 463.0629, found 463.0621. Anal. calcd. for $C_{23}H_{15}ClN_4O_3S$: C, 59.68; H, 3.27; N, 12.10; S, 6.93; found: C, 59.64; H, 3.48; N, 11.98; S, 6.84.

(E)-N′-((7-bromo-4-oxo-4H-chromen-3-yl)methylene)-3-methyl-1-phenyl-1H-thieno[2,3-c]pyrazole-5-carbohydrazide (7b) Yellow solid, m.p. 214–216 °C, Yield: 81 %. IR (KBr, cm^{-1}): 3442 (NH), 1690 (amide C=O), 1634 (pyrone C=O). ^{1}H NMR (400 MHz, DMSO-d_6, δ, ppm): 2.45 (s, 3H, CH_3), 7.32–7.76 (m, 5H, Ar–H), 7.55 (d, 1H), 7.71 (dd, 1H), 8.04 (d, 1H), 8.10 (s, 1H, thiophene-H), 8.21 (s, 1H), 8.62 (s. 1H, CH=N), 10.62 (s, 1H, NH). ^{13}C NMR (100 MHz, DMSO-d_6, δ, ppm): 13.12, 105.98, 116.08, 116.78, 117.98, 123.01, 124.62, 125.11, 125.45, 129.60, 130.50, 134.97, 138.14, 139.70, 141.50, 143.45, 145.05, 154.98, 157.0, 161.95, 163.48, 176.91. HRMS (ESI+) *m/z*: $(M + H)^+$ calcd. for $C_{23}H_{15}BrN_4O_3S$ 507.0124, found 507.0115. Anal. calcd. for $C_{23}H_{15}BrN_4O_3S$: C, 54.45; H, 2.98; N, 11.04; S, 6.32; found: C, 54.66; H, 3.09; N, 10.95; S, 6.53.

(E)-N′-((6-chloro-7-methyl-4-oxo-4H-chromen-3-yl)methylene)-3-methyl-1-phenyl-1H-thieno[2,3-c]pyrazole-5-carbohydrazide (7c) Yellow solid, m.p. 177–179 °C, Yield: 80 %. IR (KBr, cm^{-1}): 3451 (NH), 1698 (amide C=O), 1629 (pyrone C=O). ^{1}H NMR (400 MHz, DMSO-d_6, δ, ppm): 2.33 (s, 3H, CH_3), 2.47 (s, 3H, CH_3), 7.21 (s, 1H), 7.29–7.88 (m, 5H, Ar–H), 8.00 (s, 1H), 8.12 (s, 1H, thiophene-H), 8.23 (s, 1H), 8.63 (s. 1H, CH=N), 10.48 (s, 1H, NH). ^{13}C NMR (100 MHz, DMSO-d_6, δ, ppm): 13.01, 18.29, 106.03, 115.90, 116.22, 116.69, 118.08, 125.33, 128.94, 129.61, 130.55, 131.55, 133.80, 135.04, 138.10, 139.75, 143.42, 155.00, 161.97, 163.13,

176.90. HRMS (ESI+) *m/z*: $(M + H)^+$ calcd. for $C_{24}H_{17}ClN_4O_3S$ 477.0786, found 477.0770. Anal. calcd. for $C_{24}H_{17}ClN_4O_3S$: C, 60.44; H, 3.59; N, 11.75; S, 6.72; found: C, 60.74; H, 3.57; N, 11.97; S, 6.84.

(E)-N′-((6,7-dimethyl-4-oxo-4H-chromen-3-yl)methylene)-3-methyl-1-phenyl-1H-thieno[2,3-c]pyrazole-5-carbohydrazide (7d) Yellow solid, m.p. 154–156 °C, Yield: 78 %, IR (KBr, cm^{-1}): 3476 (NH), 1688 (amide C=O), 1644 (pyrone C=O). ^{1}H NMR (400 MHz, DMSO-d_6, δ, ppm):, 2.27 (s, 3H, CH_3), 2.31 (s, 3H, CH_3), 2.45 (s, 3H, CH_3), 7.16 (s, 1H), 7.64 (s, 1H), 7.32-7.74 (m, 5H, Ar–H), 8.12 (s, 1H, thiophene-H), 8.29 (s, 1H), 8.65 (s. 1H, CH=N), 10.42 (s, 1H, NH). ^{13}C NMR (100 MHz, DMSO-d_6, δ, ppm): 13.00, 17.21, 17.72, 106.05, 115.92, 116.68, 118.05, 124.01, 125.36, 129.55, 130.57, 131.58, 133.82, 135.05, 138.06, 141.21, 143.44, 149.31, 152.31, 154.66, 162.06, 163.11, 176.92. HRMS (ESI+) *m/z*: $(M + H)^+$ calcd. for $C_{25}H_{20}N_4O_3S$ 457.1332, found 457.1318. Anal. calcd. for $C_{25}H_{20}N_4O_3S$: C, 65.77; H, 4.42; N, 12.27; S, 7.02; found: C, 65.72; H, 4.45; N, 12.14; S, 6.91.

Biological methods

Antioxidant activity

2 mL of solution containing 0.2-mM freshly prepared 1,1-diphenyl-2-picryl-hydrazil (DPPH) in methanol and different concentrations of synthesized compounds (10–100 μg/mL) were prepared to perform the reaction. After incubation at room temperature for 30 min, the absorbance at 517 nm was measured spectrophotometrically [38]. A graph pad prism was used to calculate the concentration required to obtain a 50-% antioxidant effect (EC_{50}) and is compared with the butylated hydroxy toluene (BHT) standard, by performing the experiment in triplicate. DPPH radical scavenging capacity was measured by:

$$\%\,\text{scavenging activity} = A_{\text{control}} - A_{\text{test}}/A_{\text{control}} \times 100$$

A_{control} = Absorbance of the control, A_{test} = Absorbance of the test compounds

Anti-inflammatory activity

The reaction mixture consisting of 0.5 mL of 10-% human red blood cell (HRBC) suspension, 1 mL hypo saline, 1 mL of 0.2-M phosphate buffer, and 1 mL of test sample at different concentrations in normal saline was incubated at 37 °C for 30 min and centrifuged at 3000 rpm for 30 min. The hemoglobin content of the supernatant solution was estimated at 560 nm spectrophotometrically. Each experiment was performed in triplicate and distilled water used as the control in this study. EC_{50} values were determined for each compound. Where the blood control represents zero percent stability or 100 % lysis, the percentage of HRBC heamolysis was calculated by:

$$\%\text{of Heamolysis} = (\text{O.D. of Control} - \text{O.D. of Test sample}/\text{O.D. of Control}) \times 100$$

Molecular docking

Molecular docking studies were performed using the grid-based ligand docking with energetics (Glide) [39, 40] module integrated in the Schrödinger molecular modeling package (Schrödinger, Inc., USA, *version-2014–14*) installed on a Windows workstation with an Intel (R) Xenon 2.8-GHz processor and 32 GB of physical memory. It is an interactive molecular graphics program for docking calculations, studying ligand-receptor interactions and identifying possible binding sites of biomolecules. The X-ray crystal structure of cyclooxygenase-2 (COX-2) in complex with its inhibitor *diclofenac* was retrieved from the Protein Data Bank (www.rcsb.org; PDB ID: 1PXX).

First, the crystal structure was pre-processed using the *Protein Preparation Wizard* by deleting the crystallographically observed water molecules since no water molecule was observed to be conserved, correcting the mistakes in the PDB structure and optimizing the hydrogen bonds. Following this, hydrogen atoms were added to the crystal structure corresponding to pH 7.0, considering the appropriate ionization states for the acidic and basic amino acid residues. The most likely positions were selected for the –OH and –SH hydrogen atoms, protonation states and tautomers of His residues and Chi 'flip' assignments were made for Asn, Gln and His amino acid residues. Following the assignment of charge and protonation state, energy minimization with a root mean square deviation (RMSD) value of 0.30 Å was carried out using an OPLS-2005 force field to relieve the steric clashes among the residues due to addition of hydrogen atoms.

The three-dimensional (3D) structures of *N*-acylheteroaryl hydrazone (NAH) derivatives were built using the *builder* panel in Maestro followed by ligand preparation using the Ligprep module which performs addition of hydrogens, adjusting realistic bond lengths and angles, correcting chiralities, ionization states, tautomers, stereo chemistries and ring conformations. Geometry minimization was then performed on all the structures by means of the OPLS 2005 force field using a default setting (Macro Model, Schrödinger, LLC, USA) till it reached an RMSD cutoff of 0.01 Å and the resulting structures were then used for carrying out the docking study.

The receptor grid was generated to define the active site of COX-2 for docking using the *Receptor Grid Generation* panel in Glide. It uses two cubical boxes having a common centroid to organize the calculations: a larger enclosure and a smaller binding box. A Grid file was generated by defining a 14 × 14 × 14 Å box centered on the geometric centroid of the COX-2 structure to explore a large region of the enzyme structure. Default values were maintained for the van der Waals scaling while partial charges were assigned from the input structure, rather than from the force field, by selecting the *use input partial charges* option. All the *N*-acylheteroaryl hydrazone (NAH) derivatives were docked into the binding site defined using the Grid generation protocol utilizing the *extra precision* (XP) Glide

scoring function to rank the docking poses and to estimate the protein–ligand binding affinities. The Glide algorithm carries out a systematic search of positions, orientations and conformations for the ligand in the active site of the enzyme using a funnel-type approach. The output files were analyzed using Maestro's pose viewer utility.

Results and discussion

Chemistry

The synthesis of new 3-methyl-1-phenyl-1*H*-thieno[2,3-*c*]pyrazole-5-acylhydrazone derivatives (Scheme 2) was initiated from the 3-methyl-1-phenyl-1*H*-thieno[2,3-*c*]pyrazole-5-carbohydrazide **1** prepared in good yield, according to the literature procedure [41] (Scheme 1). The aldehyde function of **P** was converted to the corresponding methyl ester **Q** by cyclocondensation between 5-chloro-4-carbaldehyde **P** and methyl thioglycolate in 85 % yield. 3-Methyl-1-phenyl-1*H*-thieno[2,3-*c*]pyrazole-5-carboxylate **Q** reacted with hydrazine hydrate in methanol at reflux afforded corresponding carbohydrazide **1** in 80 % yield (Scheme 1). Finally, the new stable solid NAH compounds **3a–g**, **5a–h**, and **7a–d** were prepared in good yields by condensing key intermediate **1** with the suitable heterocyclic aldehydes in methanol using acetic acid as a catalyst (Scheme 2). All the compounds were characterized by FTIR, ^{1}H NMR, ^{13}C NMR, elemental analysis and HRMS.

The ^{1}H NMR spectrum of compound **3a** displayed a broad singlet at δ 11.89 ppm (NH) and at δ 9.02 ppm (CH=N). The IR spectrum of compound **3a** showed a significant absorption bands at 3444 and 1636 cm^{-1} assigned to –NH and amide (CONH), respectively. Its HRMS spectrum showed a molecular ion peak at 497.1504, consistent with its molecular formula $C_{25}H_{20}N_8O_2S$. In the IR spectrum of compounds **5a** and **7a**, the absorption bands at 3260 and 3448 cm^{-1} for NH stretching and at 1650 and 1704 cm^{-1} for amide stretching were observed, respectively. The ^{1}H NMR of compound **5a** showed the characteristic –NH signal at δ 11.35 ppm and the –CH=N proton at δ 9.36 ppm. Similarly, **7a** exhibited a singlet peak at δ 10.56 ppm for an NH proton and at δ 8.60 ppm related to –CH=N. The mass spectra of compounds **5a** and **7a** detected expected molecular ion peaks at 503.1656 and 463.0621, corresponding to molecular formula $C_{29}H_{22}N_6OS$ and

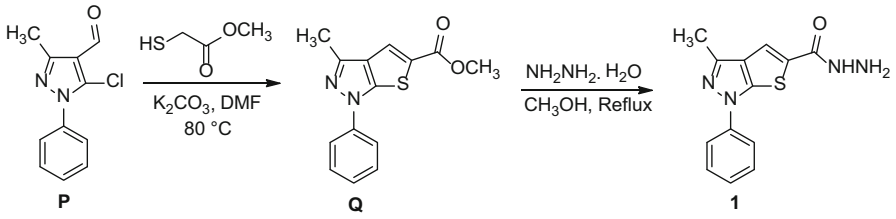

Scheme 1 3-methyl-1-phenyl-1H-thieno[2,3-*c*]pyrazole-5-carbohydrazide

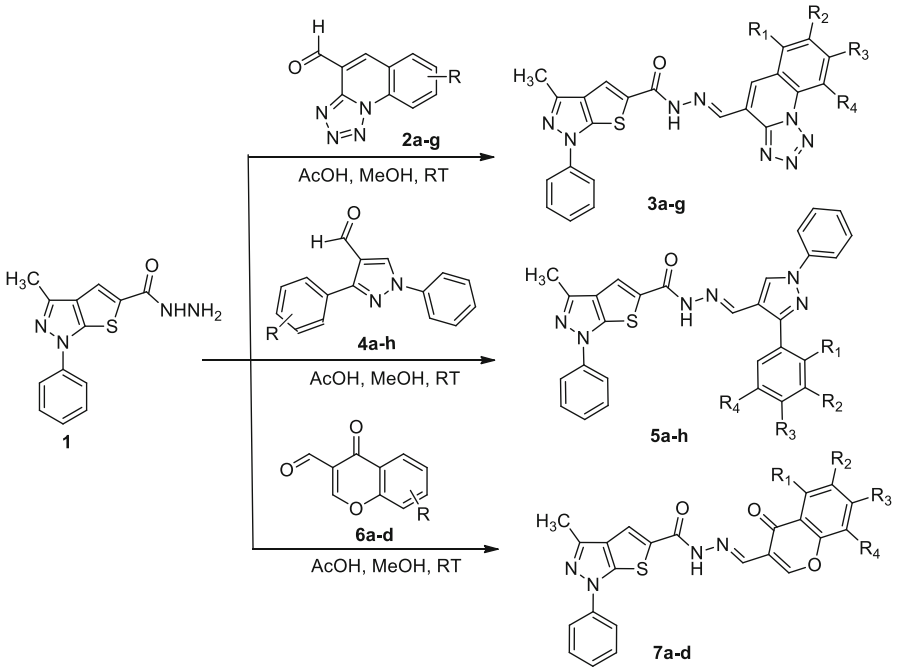

Scheme 2 Synthesis of *N*-acylhydrazone derivatives

$C_{23}H_{15}ClN_4O_3S$, respectively. All other derivatives were well proven by the spectral techniques.

Biological evaluation and in silico study

In vitro antioxidant activity

Due to the lower electron density of C=N bonds [42], hydrazones are superior radical acceptors compared to imines. So, it was thought that *N*-acylhydrazones could show better antioxidant activity. A DPPH radical scavenging method was used to evaluate the antioxidant potential of all synthesized compounds [43, 44] (Table 1). During the study of antioxidant activity of all compounds (Table 1), it has been observed that compounds **3a** ($EC_{50} = 6.00 \pm 2.36$ μg/mL) and **5c** ($EC_{50} = 7.21 \pm 0.67$ μg/mL) showed the most potent activity as compared to all other hydrazone series compounds and also compared to the standard drug BHT ($EC_{50} = 8.25 \pm 0.34$ μg/mL), while compounds **3c**, **3d**, **5b**, **5e** and **7c** showed good activity (ranging 9.32 ± 1.77–15.57 ± 4.21) as compared to other compounds of the series and less comparable to BHT.

Table 1 *In vitro* antioxidant activity (DPPH radical scavenging method) and anti-inflammatory activity (HRBC membrane stabilization method) of compounds **3a–3g**, **5a–5h** and **7a–d**

Compound	R_1	R_2	R_3	R_4	Antioxidant activity (EC_{50} ± SD) (μg/mL)	Anti-inflammatory activity (EC_{50} ± SD) (μg/mL)
3a	–H	$–OCH_2CH_3$	–H	–H	06.00 ± 2.36	77.31 ± 2.34
3b	–H	–H	–H	–H	47.00 ± 2.79	10.25 ± 1.08
3c	–H	$–OCH_3$	–H	–H	15.00 ± 1.32	45.54 ± 1.46
3d	–H	–H	$–OCH_3$	–H	12.00 ± 0.97	49.64 ± 4.22
3e	–H	$–CH_3$	–H	–H	59.99 ± 1.54	11.26 ± 2.00
3f	–H	–H	$–CH_3$	–H	51.00 ± 0.76	19.36 ± 0.97
3g	–H	–H	–H	$–CH_3$	56.63 ± 1.66	66.23 ± 1.45
5a	–H	–H	–H	–H	>100	13.23 ± 2.36
5b	–H	–H	$–NO_2$	–H	12.32 ± 1.33	54.00 ± 2.13
5c	–H	–H	$–OCH_3$	–H	07.21 ± 0.67	16.00 ± 2.19
5d	–H	–H	–F	–H	>100	52.32 ± 1.33
5e	–H	–H	–OH	–H	09.32 ± 1.77	50.13 ± 2.03
5f	–H	–H	–Cl	–H	76.09 ± 3.33	49.99 ± 1.39
5g	–H	–H	$–CH_3$	–H	57.77 ± 1.65	14.00 ± 1.26
5h	–H	–H	–Br	–H	81.34 ± 1.99	38.09 ± 0.99
7a	–H	–H	–Cl	–H	> 100	33.38 ± 0.31
7b	–H	–H	–Br	–H	19.90 ± 3.48	10.50 ± 0.99
7c	–H	–Cl	$–CH_3$	–H	15.57 ± 4.21	11.18 ± 0.15
7d	–H	$–CH_3$	$–CH_3$	–H	97.00 ± 2.64	23.00 ± 0.75
BHT	–	–	–	–	8.25 ± 0.34	–
DFS	–	–	–	–	–	11.70 ± 0.98

Values are expressed as mean ± standard deviation ($n = 3$)

BHT Butylated hydroxy toluene, *DFS* Diclofenac sodium, *SD* standard deviation

In vitro-anti-inflammatory activity

Anti-inflammatory agents act by either inhibiting lysosomal enzymes or by stabilizing lysosomal membranes, and HRBC membranes are similar to these lysosomal membrane components [45]. Hence, lysis of an HRBC membrane is taken as a measure of anti-inflammatory activity. *In vitro* anti-inflammatory activity was studied via the HRBC membrane stabilization method against the standard drug diclofenac sodium (DFS) [46] (Table 1).

As shown in Table 1, compounds **3b** ($EC_{50} = 10.25 \pm 1.08$), **7b** ($EC_{50} = 10.50 \pm 0.99$) and **7c** ($EC_{50} = 11.18 \pm 0.15$) exhibited the most potent anti-inflammatory activity as compared to all other hydrazone series compounds and standard drug DFS ($EC_{50} = 11.70 \pm 0.98$), while compounds **3e**, **3f**, **5a**, **5c** and **5g** were found to be active as compared to all other compounds and less comparable to DFS. The anti-inflammatory activity of hydrazones could be due to their binding

onto the erythrocyte membranes with subsequent alteration of the charges on the surface of the cells. This might have prevented physical interaction with aggregating agents or promote dispersal by mutual repulsion of like charges involved in the haemolysis of red blood cells [47].

Molecular docking

A molecular docking study was carried out to gain insight into molecular interactions that govern the binding of NAH derivatives with the target enzyme COX-2. Structures of NAH derivatives as well as the enzyme were kept flexible to obtain different binding conformations and the best docked complex obtained from it was analyzed in detail. The molecular docking protocol utilized in the current study was validated by extracting the native ligand *diclofenac* from the binding site and re-docking it to the binding site of COX-2. The RMSD between the original conformation of *diclofenac* and the conformation obtained from its re-docking into COX-2 structure was found to be less than 1 Å, validating the reliability and reproducibility of the docking procedure (Fig. 1).

Results of the molecular docking study have been analyzed on the basis of four main parameters- Glide score, Glide energy, non-bonded interactions (van der Waals and coulombic) and H-bonds. Considering these parameters, the binding affinity of the NAH derivatives towards COX-2 has been discussed. Ten different binding conformations were retained for each compound from docking simulations. Table 2 presents the intermolecular interaction energy values obtained from the docking calculation.

The ligands have been ranked on the basis of their Glide score and the percentage enzyme activity. Analysis of the docking poses showed that NAH derivatives got docked into the binding site of COX-2 at the same site as was observed for *diclofenac* complexed with COX-2 and, hence, could serve as a pertinent starting point for the rational design of potent COX-2 inhibitors. All the compounds

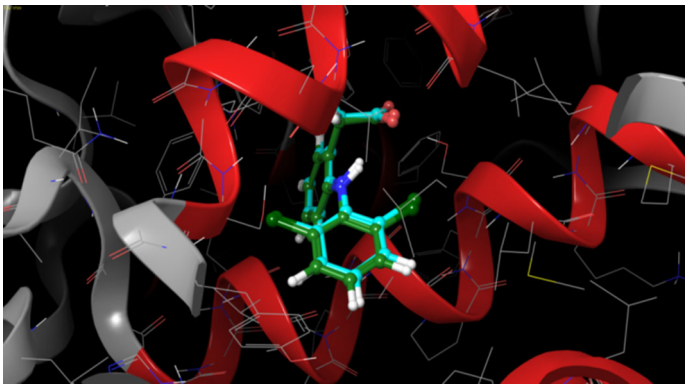

Fig. 1 Overlay of the X-ray conformation of diclofenac (*blue back-bone*) over its best docked conformation (*green back-bone*). (Color figure online)

Table 2 Quantitative analysis of the docking results- Glide score, Glide energy and non-bonded interactions (van der Waals (VDW) and electrostatic)

Compound	Glide score	Glide energy	VDW energy	Coulombic energy
3a	−6.002	−36.273	−34.989	−1.285
3b	−8.925	−59.304	−54.256	−5.048
3c	−7.255	−48.732	−45.793	−2.939
3d	−7.134	−47.392	−45.149	−2.244
3e	−8.115	−54.895	−50.175	−4.721
3f	−7.75	−50.177	−47.046	−3.131
3g	−6.294	−43.658	−41.814	−1.844
5a	−8.048	−53.584	−50.445	−3.139
5b	−6.703	−44.706	−42.607	−2.099
5c	−7.865	−52.442	−48.993	−3.449
5d	−6.933	−45.886	−43.792	−2.094
5e	−7.008	−46.615	−44.327	−2.289
5f	−7.020	−47.278	−45.093	−2.185
5g	−7.95	−52.674	−49.375	−3.299
5h	−7.359	−49.13	−46.861	−2.269
7a	−7.583	−49.931	−47.775	−2.156
7b	−8.869	−58.359	−52.808	−5.551
7c	−8.197	−55.806	−51.101	−4.704
7d	−7.656	−50.083	−47.027	−3.056
DFS	−8.077	−54.592	−50.324	−4.268

exhibited good binding affinity towards COX-2 with an average docking score of −7.05. The docking score of these ligands varied from –6.00 to −8.95, while the docking score for the native ligand *diclofenac* was found to be −8.07.

A plot of the anti-inflammatory activity expressed as EC_{50} values versus the Glide docking score of NAH derivatives is shown in Fig. 6. A significant correlation was observed between the docking scores of the docked ligands and EC_{50} values, validating that the binding site of NAH derivatives is similar to that of *diclofenac*. A per-residue interaction analysis between the protein and the NAH derivatives was performed to investigate detailed interpretations of the molecular mechanisms involved in their anti-inflammatory activity. From the ensuing docked structures, it is clear that all the NAH derivatives snugly fit into the active site of COX-2, resulting in various close contacts with the amino acid residues lining the active site. The per residue interaction analysis could also provides an explanation for the observed difference in binding affinity for these molecules. For the sake of brevity, the per-residue interaction analysis has been discussed in detail only for the most active compounds **3b**, **3e**, **7b** and **7c** (Fig. 1).

Docking of the most active compound **3b** into the active site of COX-2 showed that the inhibitor binds at the same site as the native ligand *diclofenac* with a

significantly higher binding affinity (Fig. 2). Even the Glide score for **3b** was found to be higher (−8.925) than that of diclofenac (−8.077). The per-residue interaction analysis showed that the van der Waals interactions (−54.256 kcal/mol) surpassed the electrostatic contribution (-5.048 kcal/mol) in the overall binding affinity. The overall binding energy of compound **3b** was also found to be −59.304 kcal/mol as compared to −54.592 kcal/mol observed for *diclofenac*. The higher binding affinity observed for **3b** can be explained in terms of the specific bonded and non-bonded per residue interactions with the residues comprising the active site. The compound is stabilized within the active site through extensive van der Waals contacts with Ala527 (−1.655 kcal/mol), Ile517 (−1.492 kcal/mol), Ala516 (−2.778 kcal/mol), Asp515 (−2.993 kcal/mol), Arg513 (−2.317 kcal/mol), Trp387 (−1.274 kcal/mol), Tyr385 (−1.184 kcal/mol), Tyr355 (−2.291 kcal/mol), Gly354 (−2.505 kcal/mol), Val349 (−2.395 kcal/mol), Gln192 (−4.413 kcal/mol), Thr94 (−3.642 kcal/mol) and His90 (-1.185 kcal/mol) residues. The enhanced binding affinity of **3b** can also be attributed to favorable electrostatic contacts with Arg513 (−3.031 kcal/mol), Arg433 (−1.507 kcal/mol) and Ser353 (−2.222 kcal/mol) residues lining the active site. The enzyme-inhibitor complex was further stabilized by crucial hydrogen bonding interactions observed with Ser353, Leu352 and Tyr115. These hydrogen bonds may act as "anchors", guiding the 3D orientation of the ligand in its active site, thereby facilitating the steric and electrostatic interactions.

The results obtained from molecular docking for the second most active compound **7b** showed that it binds to the target at the same site (Fig. 3) as occupied by *diclofenac* and **3b**, indicating that even this compound is mediating its activity via inhibiting COX-2. The Glide score was observed to be −8.869 with an overall binding energy of −58.359 kcal/mol. The binding affinity of **7b** was, like **3b**, found to be better than *diclofenac*. Inspection of the van der Waals and electrostatic interaction energies revealed that the compound shares higher values of van der Waals interaction energy (−52.808 kcal/mol) over the electrostatic component (−5.551 kcal/mol) in the overall binding energy. The per residue ligand interaction

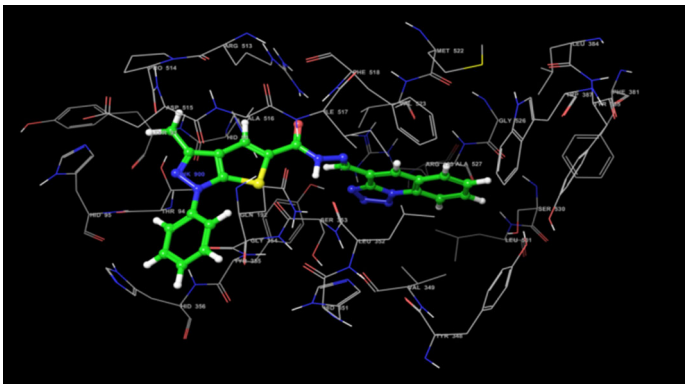

Fig. 2 Model of compound **3b** docked into the binding site of COX-2 (image shows the interactions observed with the residues within 5 Å distance of the ligand)

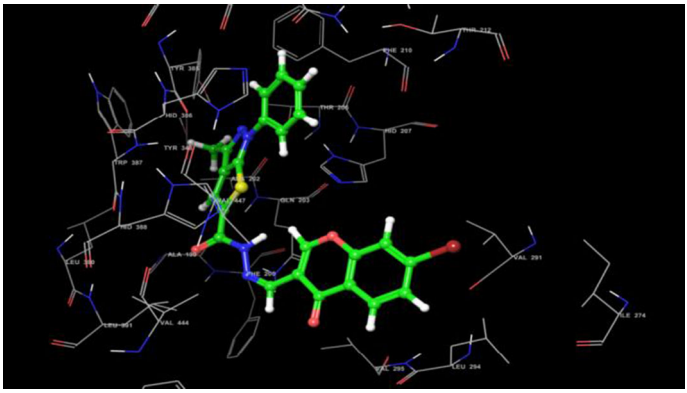

Fig. 3 Model of compound **7b** docked into the binding site of COX-2

energy distribution shows that it forms favorable van der Waals interactions with His388 (−4.793 kcal/mol), Trp387 (−1.194 kcal/mol), His386 (−4.634 kcal/mol), Tyr385 (−1.553 kcal/mol), Asn382 (−1.872 kcal/mol), Phe210 (−1.84 kcal/mol), His207 (−2.709 kcal/mol), Thr206 (−1.358 kcal/mol), Gln203 (−7.636 kcal/mol) and Ala202 (−1.714 kcal/mol). It also showed significant electrostatic interactions with His388 (−1.831 kcal/mol), His207 (−1.613 kcal/mol), Thr206 (−1.937 kcal/-mol) and Gln203 (−1.98 kcal/mol) along with a crucial hydrogen bonding interactions via Thr206 to anchor the ligand at its active site in the enzyme.

The Glide score for **7c** (Fig. 4) was −8.197 with an overall binding energy of −55.806 kcal/mol. Wherein the contribution from van der Waals interaction was seen to be −51.101 kcal/mol while coulombic interaction contributed −4.704 kcal/-mol, which is slightly better than *diclofenac*. Significant van der Waals interactions were observed with His388 (−3.139 kcal/mol), Trp387 (−1.188 kcal/mol), His386 (−2.365 kcal/mol), Tyr385 (−1.066 kcal/mol), Asn382 (−1.188 kcal/mol), Phe210 (−1.069 kcal/mol), His207 (−1.091 kcal/mol), Thr206 (−1.041 kcal/mol) and

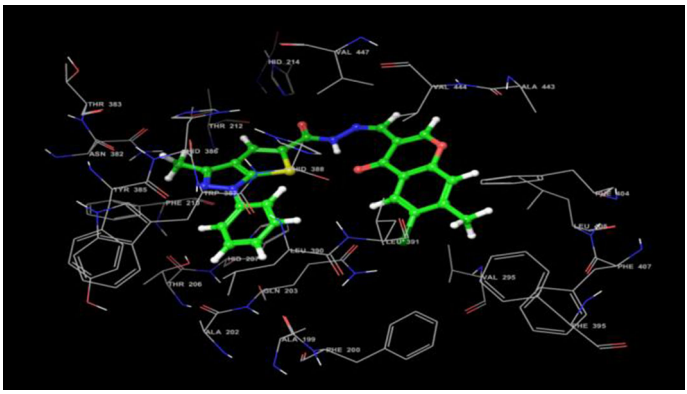

Fig. 4 Model of compound **7c** docked into the binding site of COX-2

Gln203 (−3.927 kcal/mol) residues in the active site. Further, it also formed favorable electrostatic interactions with Gln203 (−1.127), Phe210 (−1.185) and His207 (−1.114) residues in the active site. However, no significant hydrogen bonding interactions were observed.

Finally, docking of the fourth most active compound **3e** (Fig. 5) into COX-2 produced a relatively lower Glide score (−8.115) compared to compound **3b**, **7b** and **7c** but better than *diclofenac,* which is in harmony with experimentally observed activity for these compounds. The overall binding energy of the compound was found to be −54.895 kcal/mol wherein the contribution of van der Waals components was found to be more prevalent (−50.175) than the electrostatic interaction energy (−4.721 kcal/mol). It forms an extensive chain of favorable van der Waals interactions with Ser530 (−1.119 kcal/mol), Ala527 (−1.189 kcal/mol), Leu525 (−1.23 kcal/mol), Val523 (−1.89 kcal/mol), Phe518 (−3.757 kcal/mol), Ile517 (−1.334 kcal/mol), Asp515 (−1.476 kcal/mol), Arg513 (−2.166 kcal/mol), Tyr385 (−1.077 kcal/mol), Tyr355 (−2.03 kcal/mol), His351(−1.00 kcal/mol), Val349 (−2.202 kcal/mol) and Thr94 (−3.272 kcal/mol) residues in the active site of COX-2. Additionally, favorable electrostatic interactions were also observed with Arg513 (−1.253 kcal/mol), Leu352 (−2.607 kcal/mol), Asp190 (−1.705 kcal/mol) and Arg120 (−3.441 kcal/mol) along with a H-bond interaction with the active site via Leu352 contributing to stabilization of the ligand–enzyme complex.

Overall, the molecular docking results obtained for the NAH derivatives were found to be in agreement with the observed anti-inflammatory activity. The per-residue ligand-receptor interaction analysis showed that the primary driving force for mechanical interlocking was the steric complementarity between the docked ligands and the active site of the enzyme, as evidenced from the relatively higher contribution of van der Waals interaction over other components contributing to the overall binding scores. The binding pattern predicted by docking complemented with a detailed per residue interaction analysis may facilitate the rational design of anti-inflammatory leads (Fig. 6).

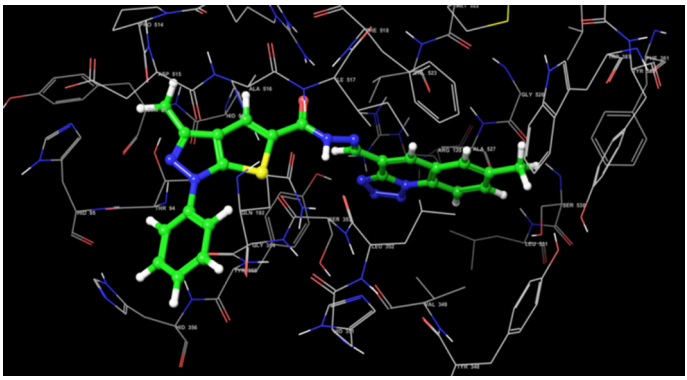

Fig. 5 Model of compound **3e** docked into the binding site of COX-2

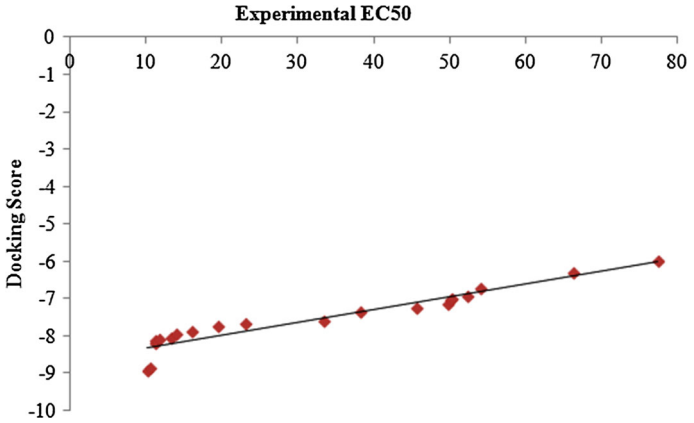

Fig. 6 Correlation plot of anti-inflammatory (EC_{50}) versus the Glide docking score for NAH derivatives

Table 3 Pharmacokinetic properties important for good oral bioavailability of compounds **3a–3g**, **5a–5h** and **7a–d**

Compound	% ABS	Volume (A^3)	TPSA (A^2)	NROTB	HBA	HBD	Log *P*	Lipinski's Violations	Drug likeness model score
Rule	–	–	–	–	<10	<5	≤5	≤1	
3a	34.93	417.2	111.6	6	10	1	4.4	0	0.22
3b	20.30	374.8	102.3	4	9	1	3.9	0	0.24
3c	29.13	400.4	111.6	5	10	1	4.0	0	0.26
3d	26.03	391.4	102.3	4	9	1	4.4	0	0.28
3e	26.03	391.4	102.3	4	9	1	4.4	0	0.03
3f	26.03	391.4	102.3	4	9	1	4.3	0	0.04
3g	29.13	400.4	111.6	5	10	1	4.0	0	0.29
5a	42.11	438.0	77.11	6	7	1	5.6	2	0.26
5b	50.14	461.3	122.9	**7**	10	1	5.6	2	0.18
5c	50.90	463.5	86.3	7	8	1	5.7	2	0.51
5d	43.80	442.9	77.1	6	7	1	5.8	2	0.69
5e	44.87	446.0	97.3	6	8	2	5.1	2	0.79
5f	46.76	451.5	77.1	6	7	1	6.3	2	0.81
5g	47.80	454.5	77.1	6	7	1	6.1	2	0.40
5h	48.25	455.8	77.1	6	7	1	6.4	2	0.51
7a	19.34	372.0	89.4	4	7	1	4.8	0	0.27
7b	20.85	376.4	89.4	4	7	1	4.9	1	0.08
7c	25.06	388.6	89.4	4	7	1	5.1	1	0.02
7d	26.10	391.6	89.4	4	7	1	4.9	0	−0.05

% ABS percentage of absorption; *MW* molecular weight; *TPSA* topological polar surface area; *NROTB* number of rotatable bonds; *Log P* logarithm of compound partition coefficient between *N*-octanol and water; *HBA* number of hydrogen bond acceptors; *HBD* number of hydrogen bond donors

In silico absorption, distribution, metabolism, excretion (ADME) and drug likeness analysis

A computational study of all the synthesized compounds was performed for the prediction of absorption, distribution, metabolism, and excretion (ADME) properties using a Molinspiration online property calculation toolkit [48], and the values are presented in Table 3. Some compounds showed good absorption (% ABS) [49], in the range of 42.11–50.90 %. Furthermore, compounds **3a**, **3d**, **3e**, **3f**, **7a**, **7b** and **7d** are in good agreement with Lipinski's rule of five and, thus, show good drug-like properties [50, 51]. A molecule likely to be developed as an orally active drug candidate should show no more than one violation of the above shown criteria. Compounds **3a**, **3d**, **3e**, **3f**, **7a**, **7b** and **7d** followed the criteria for an orally active drug and, therefore, these compounds may have a good potential for eventual development as oral agents. An overall drug-likeness was studied using molsoft online and from the data, most of the compounds have shown a good model score. Hence, these molecules showed good drug-like properties.

Structure activity relationship (SAR)

The results of the antioxidant and anti-inflammatory screening confirmed some specific and remarkable facts about the structure activity relationship (SAR) of the synthesized molecules, which could help us to understand a possible pharmacophoric benefactor for these series. The variation and dependence of the activity profile of molecules have shown the dependence on structural variations in molecules. The important thing is to determine the SARs.

*Effect of absence of the substituent on the quinoline ring (**3a–3g**)* The presence of the quinoline ring **3b** without any substitution does not make the molecule specifically active towards antioxidant activity, but it has shown the highest potent anti-inflammatory activity (10.25 ± 1.08 μg/mL) of all the studied compounds. This indicates the effect of lack of substitution on tetrazolo[1,5-*a*]quinoline.

*Effect of an electron donating alkoxy and alkyl group on the phenyl ring (**3a–3g**)* The methoxy and ethoxy group and its position to quinoline ring have an essential role in determined the antioxidant and anti-inflammatory activities. Substitution of the ethoxy group on quinoline ring **3a** make the molecule exclusively active towards potent DPPH radical scavenging activity. While substitution of methoxy group **3c** and **3d** makes the molecule active for antioxidant activity. This clearly indicates that these two groups are favorable regarding the development of broad spectrum molecule active against antioxidant activity. In the next, the screening data clearly reveals impact of the position of methyl group such that the substitution of methyl group at 7, 8 position (**3e** and **3f** resp.) has shown good anti-inflammatory activity and at 9 position (**3g**) does not show any response to the activity.

*Effect of the substituent at the para-position on the phenyl ring (**5a–5h**)* The compound without any substitution on the phenyl ring (**5a**) has shown good anti-

inflammatory activity, which points out again the effect of the absence of the substitution on the phenyl ring. The substitution of an electron-withdrawing nitro group (**5b**) and electron-donating groups (**5c–5h**) at the *para* position on the phenyl ring clearly show that the electron donating methoxy group **5c** (active for antioxidant and anti-inflammatory activity), **5e** (active against DPPH radicals), **5g** (active for anti-inflammatory activity) and an electron withdrawing group (active against DPPH radicals) may be good for the development of a broad spectrum of antioxidant and anti-inflammatory molecules.

*Combined effect of a halo and a methyl group (**7a–d**)* From the obtained data, compound **7c** with a *bromo-* and *methyl* group showed more potency compared to other compounds of the series. This indicates that such a modification increases the molecule's potency against oxidants and inflammatory agents.

Conclusions

Three new series of 3-methyl-1-phenyl-1*H*-thieno[2,3-*c*]pyrazole-5-carbohydrazide derivatives with remarkable antioxidant and anti-inflammatory activities have been prepared. Compounds **3a** and **5c** showed the most significant antioxidant activity among the series with them being comparable to the BHT standard, while compounds **3a**, **7b**, **7c and 3e** showed promising anti-inflammatory activity comparable to DFS. This observed anti-inflammatory activity trend was further confirmed by molecular docking studies with respect to the binding energy of these NAH derivatives towards the COX-2 enzyme. The binding mode predicted for these compounds could establish a link between their binding affinity and the observed biological activity, thereby providing insights into specific bonded and non-bonded interactions governing the activity. Furthermore, ADME parameters predicted for these compounds showed good drug-like properties and can be developed as an oral drug candidate. In conclusion, **3a**, **3d**, **3e**, **3f**, **7a**, **7b** and **7d** compounds from these present series can be further optimized and developed as lead molecules. Further biological evaluation to define the mode of action as well as study of the isoenzyme inhibitory potency to assess the full potential of hydrazones is warranted.

Acknowledgments The author P. S. M. thanks the University Grants Commission, New Delhi, India, and M. D. N. thanks the Council of Scientific and Industrial Research, New Delhi, India for providing a senior research fellowship, and also thanks the Department Head of the Department of Chemistry, Dr. Babasaheb Ambedkar Marathwada University, Aurangabad, Maharashtra for providing laboratory facilities. We are also thankful to the Haffkine Research Institute, Mumbai for providing biological activities.

References

1. Z. Liu, Chem. Rev. **110**, 5675 (2010)
2. T.B.L. Kirkwood, S.N. Austad, Nature **408**, 233 (2000)
3. T. Finkel, N.J. Holbrook, Nature **408**, 239 (2000)
4. J. Scholz, C. Woolf, Nat. Neurosci. **5**, 1062 (2002)

5. L. Bertolacci, E. Romeo, M. Veronesi, P. Magotti, C. Albani, M. Dionis, C. Lambruschini, R. Scarpelli, A. Cavalli, M.D. Vivo, D. Piomelli, G. Garau, J. Am. Chem. Soc. **135**, 22 (2013)
6. M.D. Mullican, M.W. Wilson, D.T. Connor, C.R. Kostlan, D.J. Schrier, R.D. Dyer, J. Med. Chem. **36**, 1090 (1993)
7. K.M. Amin, M.M. Kamel, M.M. Anwar, M. Khedr, Y.M. Syamb, Eur. J. Med. Chem. **45**, 2117 (2010)
8. R.G. Marie, Am. J. Med. **100**, 611 (1996)
9. A.T. Florence, P.U. Jani, Drug Saf. **10**, 233 (1994)
10. G.R. Lipscomb, W.D. Rees, Aliment. Pharmacol. Ther. **10**, 133 (1996)
11. R. Grahame, Int. J. Clin. Pract. **61**, 1959 (2007)
12. A. Detsi, D. Bouloumbasi, K.C. Prousis, M. Koufaki, G. Athanasellis, G. Melagraki, A. Afantitis, O. Igglessi-Markopoulou, C. Kontogiorgis, D.J. Hadjipavlou-Litina, J. Med. Chem. **50**, 2450 (2007)
13. A. Roussin, V.L. Cabec, M. Lonchampt, J. De Naday, E. Canet, I.M. Parini, Eur. J. Pharmacol. **322**, 91 (1997)
14. Q. Liu, K. Suzuki, S. Kudo, M. Yamada, K. Kowatari, T. Umeda, S. Nakaji, K. Sugawara, Food Chem. Toxicol. **38**, 423 (2000)
15. L. Flohe, R. Beckman, H. Giertz, G. Loschen, Oxygen centered free radicals as mediators of inflammation, in *Oxidative stress*, ed. by H. Sies (Academic Press, London, 1985), pp. 403–435
16. M. Sugiura, S. Kobayashi, Angew. Chem. Int. Ed. **44**, 5176 (2005)
17. G.K. Friestad, Eur. J. Org. Chem. **15**, 3157 (2005)
18. I. Akritopoulou-Zanze, D. Darczak, K. Sarris, K.J. Huth, D. Song, E. Johnson, Y. Gia, Bioorg. Med. Chem. Lett. **16**, 96 (2006)
19. A. Bigot, F. Clerc, G. Doerflinger, S. Mignani, H. Minoux, Patent U. S. 20050026984, 2005
20. J.C. Carry, G. Doerflinger, A. Bigot, D.B. Damour, F. Clerc, Patent WO2006056697, 2006
21. C. Barberis, J.C. Carry, G. Doerflinger, D.B. Damour, F. Clerc, Patent WO2006092510, 2006
22. G. Doerflinger, J.C. Carry, Patent WO2008015340, 2008
23. R. Silverman, Patent WO2007127212, 2007
24. K. Yamaoka, M. Goto, M. Murakawa, R. Yoshioka, Y. Tanaka, H. Inoue, H. Murafuji, S. Kanki, Y. Hayashi, K. Nagahira, A. Ogata, T. Nakatsuka, Y. Fukuda, Eur. J. Pharmacol. **613**, 163 (2009)
25. K. Kadoshima-Yamaoka, M. Murakawa, M. Goto, Y. Tanaka, H. Inoue, H. Murafuji, A. Nagahira, Y. Hayashi, K. Nagahira, K. Miura, T. Nakatsuka, K. Chamoto, Y. Fukuda, T. Nishimura, Immunol. Lett. **122**, 193 (2009)
26. D.E. John, B. Hartzoulakis, S. Edwards, Patent WO2013072693 A1, 2013
27. G. Liu, J. Xu, M. Geng, R. Xu, R. Hui, J. Zhao, Q. Xu, H. Xu, J. Li, Bioorg. Med. Chem. **18**, 2864 (2010)
28. K.M. Khan, N. Ambreen, U.R. Mughal, S. Jalil, S. Perveen, M.I. Choudhary, Eur. J. Med. Chem. **45**, 4058 (2010)
29. A.A. Bekhit, O.A. El-Sayed, E. Aboulmagd, J. Park, Eur. J. Med. Chem. **39**, 249 (2004)
30. P. Hernandez, M. Cabrera, M. Lavaggi, L. Celano, I. Tiscornia, T. Costa, L. Thomson, M. Fogolin, A.P. Miranda, L.M. Lima, E.J. Barreiro, M. Gonzalez, H. Cerecetto, Bioorg. Med. Chem. **20**, 2158 (2012)
31. A.G. El-Sehemi, S. Bondock, Y.A. Ammar, Med. Chem. Res. **23**, 827 (2014)
32. A.A. Bekhit, H.T.Y. Fahmy, Arch. Pharm. Pharm. Med. Chem. **336**, 111 (2003)
33. C. Gill, G. Jadhav, M. Shaikh, R. Kale, A. Ghawalkar, D. Nagargoje, M. Shiradkar, Bioorg. Med. Chem. Lett. **18**, 6244 (2008)
34. G.R. Jadhav, M.U. Shaikh, R.P. Kale, M.R. Shiradkar, C.H. Gill, Eur. J. Med. Chem. **44**, 2930 (2009)
35. R.S. Joshi, P.G. Mandhane, S.D. Diwakar, S.K. Dabhade, C.H. Gill, Bioorg. Med. Chem. Lett. **20**, 3721 (2010)
36. O. Prakash, K. Pannu, R. Naithani, H. Kaur, Synth. Commun. **36**, 3479 (2006)
37. K.M. Khan, N. Ambreen, S. Hussain, S. Perveen, M.I. Choudhary, Bioorg. Med. Chem. **17**, 2983 (2009)
38. T. Hatano, H. Kagawa, T. Yasuhara, T. Okuda, Chem. Pharm. Bull. **36**, 2090 (1988)
39. R.A. Friesner, J.L. Banks, R.B. Murphy, T.A. Halgren, J.J. Klicic, D.T. Mainz, M.P. Repasky, E.H. Knoll, M. Shelley, J.K. Perry, D.E. Shaw, P. Francis, P.S. Shenkin, J. Med. Chem. **47**, 1739 (2004)
40. T.A. Halgren, R.B. Murphy, R.A. Friesner, H.S. Beard, L.L. Frye, W.T. Pollard, J.L. Banks, J. Med. Chem. **47**, 1750 (2004)
41. P.S. Patil, S.B. Kanawade, D.C. Bhavsar, P.S. Nikam, S.A. Gangurde, R.B. Toche, J. Het. Chem. **51**, 368 (2014)

42. G.K. Friestad, Tetrahedron **57**, 5461 (2001)
43. L. Yu, J. Agric. Food Chem. **49**, 3452 (2001)
44. A.H. Kilclgil, T. Coban, M. Tuncbilek, B. Can-Eke, O.B. Dundar, R. Ertan, M. Iscan, Arch. Pharm. Res. **27**, 610 (2004)
45. Y. Nagaharikal, V. kalyani, S. Rasheed, J. Acute Dis. **2**, 156 (2013)
46. J. Mahimaidoss, C. Antony, A.R. Vincent, J. Pharm. Res. **6**, 188 (2013)
47. R. Perumal, A. Ramasamy, Eur. J. Med. Chem. **46**, 4687 (2011)
48. Molinspiration Chemoinformatics, http://www.molinspiration.com/cgi-bin/properties 2014
49. Y. Zhao, M.H. Abraham, J. Lee, A. Hersey, N.C. Luscombe, G. Beck, B. Sherborne, I. Cooper, Pharm. Res. **19**, 1446 (2002)
50. C.A. Lipinski, L. Lombardo, B.W. Dominy, P.J. Feeney, Adv. Drug Deliv. Rev. **46**, 3 (2001)
51. P. Ertl, B. Rohde, P. Selzer, J. Med. Chem. **43**, 3714 (2000)